Vortex phase diagram in weakly pinned $Rh_{17}S_{15}$

2009 J. Phys.: Conf. Ser. 150 052183

(http://iopscience.iop.org/1742-6596/150/5/052183)

Journal of Physics: Conference Series **150** (2009) 052183 doi:10.1088/1742-6596/150/5/052183

Vortex phase diagram in weakly pinned $Rh_{17}S_{15}$

HR Naren, A Tamizhavel, S Ramakrishnan and AK Grover

DCMP&MS, Tata Institute of Fundamental Research, Mumbai - 400005, India.

E-mail: ramky@tifr.res.in

Abstract. A vortex phase diagram of the strongly correlated superconductor $Rh_{17}S_{15}$ has been constructed via exploration of the anomalous variations in critical current density extracted from ac and dc magnetization measurements. The isofield in-phase ac susceptiblity data reveal the presence of multiple steps at different fields. The dc magnetisation hysteresis loops show the presence of a very broad fishtail commencing deep inside the mixed state and lasting upto H_{c_2}. We have also analysed the scan rate dependence of the hysteresis width in the vibrating sample magnetometer data with a view to distinguish between the different possible order-disorder transformations in the flux line lattice.

1. Introduction

Determining the vortex phase diagram is a very important aspect of characterizing type II superconductors. In disorder-free perfect crystals of conventional Type II superconductors, the loci of $H_{c1}(T)$ and $H_{c2}(T)$ are the only features in a vortex phase diagram. Whereas, with disorder (i.e., pinning), a richer phase diagram is anticipated. Peak effect and Second Magnetization Peak (SMP) are two anomalies that have been observed in weakly pinned samples of type II superconductors. The Peak effect phenomenon relates to a peak in the J_c, which is a consequence of an eventual collapse in the elasticity of the vortex lattice close to H_{c2}. SMP anomaly, typically ocurring much deeper in the vortex state, is usually considered to be pinning induced. This is also sometimes referred to as the Fishtail effect.

The mineral $Rh_{17}S_{15}$ (known as Miassite) was first synthesised by Matthias et al [1] and found to be superconducting. It has a cubic (Pm3m) structure and contains two formula units in a unit cell. Recently, some of us [2] demonstrated that the superconductivity ($T_c \approx 5.4$ K) is of strongly correlated nature. One of the striking properties we found was the remarkably high H_{c2} in the compound ($H_{c2} \approx 11$ T at T = 3 K). Also, the H_{c1} and H_{c2} show non-BCS like curvature near $T_c(0)$, a further evidence of unconventional superconductivity.

2. Experimental

Our polycrystalline sample [2] is porous and brittle and has a RRR of around 7.2. Isothermal M-H loops were recorded on a 12T Vibrating Sample Magnetometer (VSM) (Oxford Instruments). Low field Isothermal M-H scans for H_{c1} were done on a commercial SQUID magnetometer (Quantum Design Inc., model MPMS7). Isofield ac susceptibility scans were made on a home-made mutual-inductance bridge based susceptometer [6]. Scan rate dependence studies were done on a SQUID-VSM (Quantum Design Inc.) with field ramp rates ($\dot{H}=\frac{dH}{dt}$) ranging from 5 Oe/sec to 700 Oe/sec.

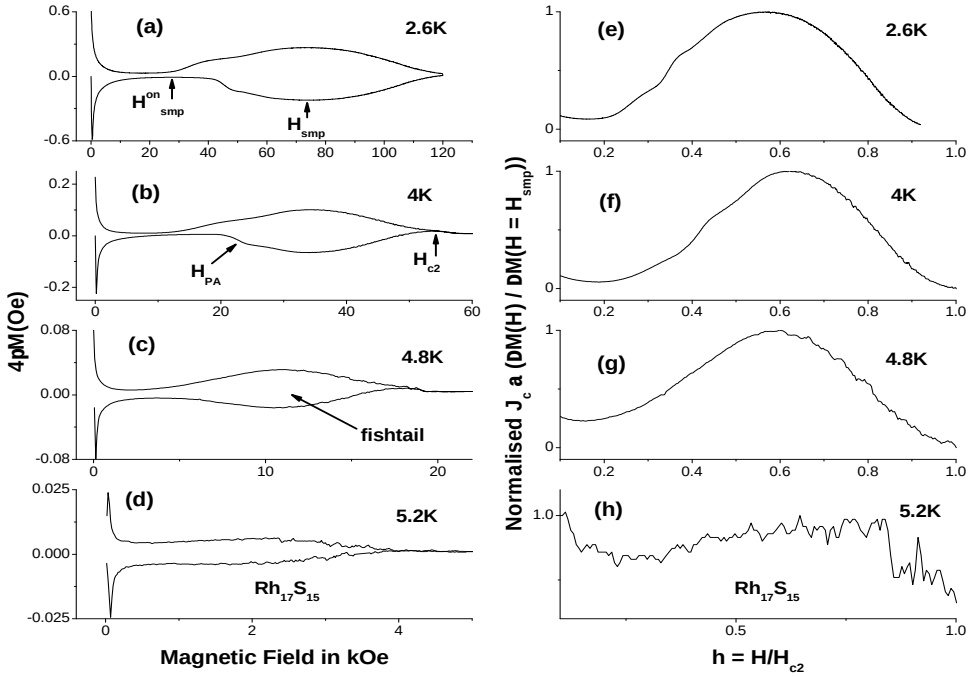

Figure 1. Panels (a) to (d) contain M-H loops and panels (e) to (h) contain the corresponding normalised j_c(h) versus normalised field (h) in $Rh_{17}S_{15}$.

3. Results and Discussions

3.1. Isothermal M-H measurements (SQUID data)

Determining H_{c1}(T) always has issues in type II superconductors. But, nevertheless, we adopt a strategy suggested by M. Naito et al [5] in determining a value for H_{c1}. We calculate a quantity δM which is the difference between the low field magnetization of the sample (corrected for demagnetisation) and that of a perfect diamagnet. δM goes as the square of the equilibrium flux density in the sample. Then we plot $(\delta M)^{1/2}$ versus H and take the value of H at which the graph takes off from zero consistently as H_{c1}. The locus of H_{c1}(T) has been plotted later in the phase diagram (Figure 5).

3.2. Isothermal M-H measurements (VSM data)

Figure 1 shows a select few isothermal two-quadrant M-H loops amongst the many measured on the VSM. As the field is ramped up, an initial sharp decrease in magnetisation followed by a turnaround constitutes the first magnetization peak relating to the penetration of flux in the interior of the sample. Beyond this, the magnetisation loop opens up again to yield an anomaly known as the Second Magnetization Peak or the Fishtail. When the field is ramped down, owing to pinning, the magnetisation changes sign and the features mentioned earlier are repeated in the top quadrant. After the loop closes, the field at which the magnetisation becomes close to zero has been taken as H_{c2}.

Using prescriptions of Bean's critical state model the width of the loop at any field can be related to the J_c at that field. Hence, in Figure 1, we have also plotted the widths of the loops (normalised to the width at the peak position of the fishtail anomaly) versus field (normalised with H_{c2}). We have identified the field values H^{on}_{smp} at which the hysteresis width starts to increase. Note that the normalised width of the SMP anomaly from h^{on}_{smp}(=H^{on}_{smp}/H_{c2}) to h = 1 is the same in all the normalised curves, it is around 0.8 in width. Also noticable is a small undulation in normalised width at h ≈0.35 in the 2.6K and 4K loops. We shall call it

a Precursor Anomaly (PA) meaning a precursor to the peak position of the SMP anomaly. It should be noted that in the M-H loops at 4.8K and above this, PA is not distinguishable.

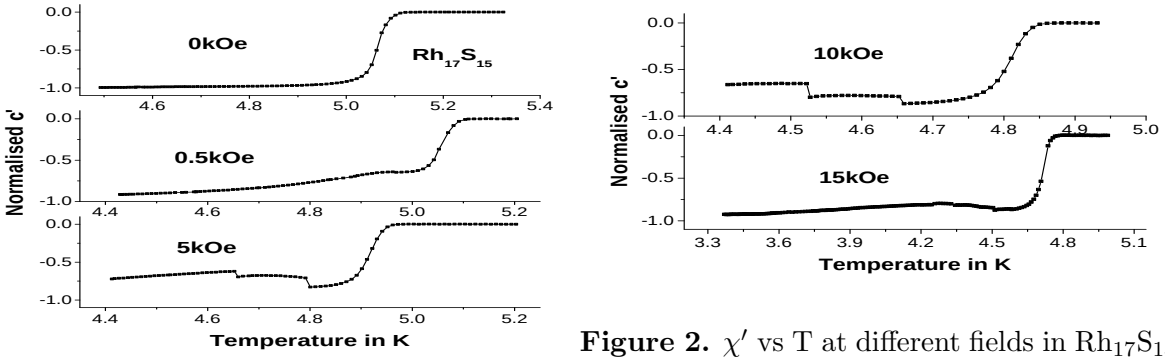

Figure 2. χ' vs T at different fields in $Rh_{17}S_{15}$.

3.3. Isofield ac susceptibility measurements
The isofield in-phase χ' vs T scans are presented in Figure 2. As we can see, the zero field χ' is featureless. In the 500 Oe run we see a monotonic increase in χ' upto 4.9K after which there is a minor dip and then we have the transition. In the 5kOe (10kOe) run we see two jumps at around 4.65K (4.52K) and 4.8K (4.66K). In the 15kOe run we see a dip at 4.5K. When we look back at our isothermal M-H data where we noted the field values of H^{on}_{smp} and H_{PA}, we see a correlation between them and the features in these isofield scans. For instance, the dip in the 15kOe scan at 4.5K can be correlated to the PA in the 4.5K fishtail which happens at around 15kOe. Similarly the jumps at 4.52K and 4.66K in the 10kOe scan can be correlated to the H^{on}_{smp} at 4.54K and the H_{PA} of the fishtail at 4.68K. These correlations indicate that H^{on}_{smp} and H_{PA} are significant places where changes occur in the vortex phase of our compound. Hence, we mark the loci of these features in our phase diagram collated in Figure 5.

3.4. Isothermal ramp rate dependence of M-H curves (SQUID-VSM data)
We performed all the measurements at 4K with ramp rates varying from 5 Oe/sec to 700 Oe/sec. Also, we have considered the curves in the field ramp-up quadrant only. So we have made an analysis of our data using one half of the hysteresis width which should again be proportional to $J_c(H)$. We see that the undulation (PA) we observed earlier is present in these curves as well. But, interestingly, this feature has a clear dependence on the ramp-rate. The PA is most distinct at a ramp rate of 50 Oe/sec and becomes progressively less noticeable away from this ramp rate on both the lower and higher side. This seems to suggest that a ramp rate of around 50 Oe/sec is most suitable for observing the reorganisation of disordered vortices injected into the sample that we believe causes this PA.

In Figure 3 we have plotted J_c versus inverse scan rate at various chosen fields. This plot gives us an idea of the temporal behaviour of the vortex state at various field values since the inverse scan rate is like time [4]. The J_c values have been normalised with the respective values of J_c at the highest scan rate. Note that the temporal decay of J_c increases monotonically from low fields upto H^{on}_{smp} (=14kOe) after which it decreases monotonically till H_{smp} (=32kOe). Further, it again increases monotonically till the SMP ceases close to H_{c2}. This implies that the vortices find it easier to settle into a stationary state at the peak of the SMP rather than on its either side. We have also calculated the parameter 'S' ($= \left|\frac{dlog(J_c)}{dlog\dot{H}^{-1})}\right|_{\dot{H}^{-1}\to\infty}$) proposed in [3] which is supposed to represent the normalised decay rate of J_c at larger times (slowest scan rate). In Figure 4 we have plotted this 'S' parameter versus h. The 'S' parameter decreases from h^{on}_{smp} to h_{smp} and then increases towards h = 1. When compared with a similar analysis [4] on 2H-$NbSe_2$ and $Ca_3Rh_4Sn_{13}$, we see that the main difference is in the presence of both the Peak effect and SMP in their data, as opposed to only SMP in ours.

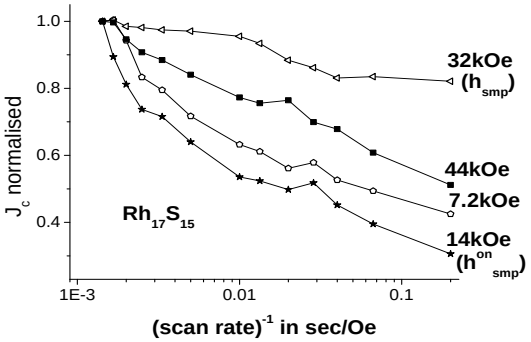

Figure 3. Normalised J_c versus inverse scan rate at various fields in $Rh_{17}S_{15}$.

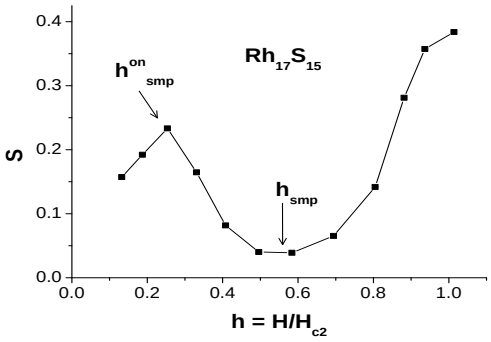

Figure 4. 'S' parameter versus h at the slowest scan rate in $Rh_{17}S_{15}$.

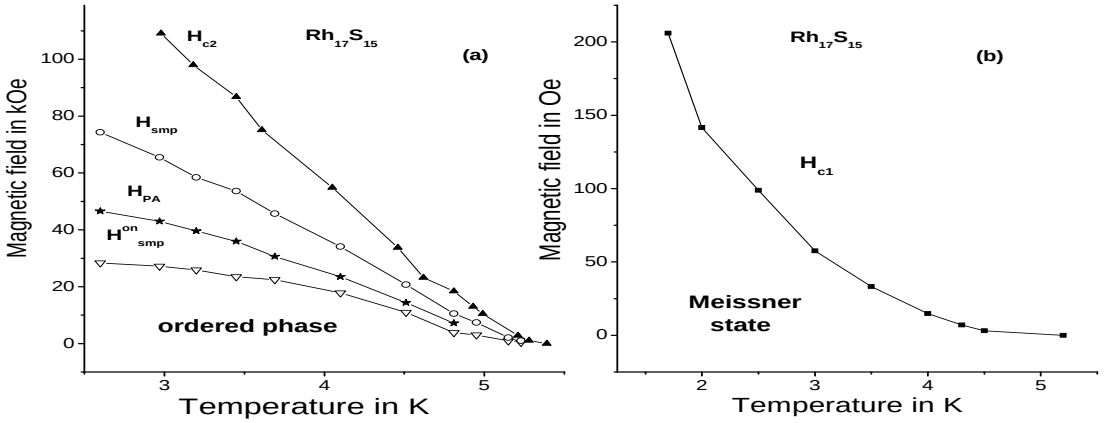

Figure 5. The vortex phase diagram of $Rh_{17}S_{15}$. H_{c1}(T) is plotted separately in panel (b) for clarity.

4. Summary and Conclusions

Figure 5 shows the vortex phase diagram of $Rh_{17}S_{15}$. We have marked the field values of H^{on}_{smp}, H_{PA} and H_{smp} alongwith H_{c2} at various temperatures. We interpret the phase diagram as follows. From lower fields upto H^{on}_{smp} the vortices enter the sample and settle in progressively more ordered configurations. The variation of 'S' versus h in Figure 4 implies that from H^{on}_{smp} till the H_{smp} the vortex state becomes more disordered and pinning-dominated. In between, at the PA feature, there is a reorganisation of the vortices. From the H_{smp} till H_{c2} the disordered vortex state could heal, i.e., it becomes better ordered and elasticity-dominated as compared to that in the preceding interval (i.e., H^{on}_{smp} to H_{smp}).

4.1. Acknowledgements

We acknowledge V. Sasidevan for participation in some of the experiments.

5. References

[1] Matthias B T, Corenzwit E and Miller C E 1954 *Phys. Rev.*, **93** 1415.
[2] Naren H R, Tamizhavel A, Nigam A K and Ramakrishnan S 2008 *Physical Review Letters*, **100** 026404.
[3] Pust L 1990 *Superconductor Science and Technology*, **3** 598.
[4] Thakur A D, Pal D, Higgins M J, Ramakrishnan S and Grover A K 2007 *Physica C*, **466** 181.
[5] Michio Naito et al 1990 *Phys. Rev.* B, **41** 4823.
[6] Ramakrishnan S, Sundaram S, Pandit R S and Girish Chandra 1985 *J. Phys, E: Sci. Instrum.* **18** 650.